Hybrid Design for Advanced Magnetic Recording Media: Combining Exchange-Coupled Composite Media with Coupled Granular Continuous Media

P. Chureemart,[1] R. F. L. Evans,[2] R. W. Chantrell,[2] P.-W. Huang,[3] K. Wang,[3] G. Ju,[3] and J. Chureemart[1,*]

[1]*Computational and Experimental Magnetism Group, Department of Physics, Mahasarakham University, Mahasarakham 44150, Thailand*

[2]*Department of Physics, University of York, York YO10 5DD, United Kingdom*

[3]*Seagate Technology, Fremont, California 94538, USA*

(Received 31 January 2017; revised manuscript received 8 June 2017; published 21 August 2017)

In order to enhance the performance of advanced granular recording media and understand the physics behind the mechanism of the reversal process, an atomistic spin-dynamics simulation is used to investigate theoretically the magnetic properties and the magnetization-reversal behavior for a composite media design. This model allows us to investigate the effect of the magnetostatic interaction and inter- and intralayer exchange coupling for a realistic system. The composite granular medium investigated consists of hard and soft composite layers in which the grains are well segregated with a continuous capping layer deposited to provide uniform exchange coupling. We present a detailed calculation aimed to reveal the reversal mechanism. In particular, the angular dependence of the critical field is investigated to understand the switching process. The calculations show a complex reversal mechanism driven by the magnetostatic interaction. It is also demonstrated, at high sweep rates consistent with the recording process, that thermal effects lead to a significant and irreducible contribution to the switching field distribution.

DOI: 10.1103/PhysRevApplied.8.024016

I. INTRODUCTION

Hard disk drives with high areal density and low cost are a significant requirement in the marketplace. It is a technical and scientific challenge for hard drive technology. In order to achieve the required high capacity, the key factor to fulfill this aim is reducing the grain size as much as possible ($D < 7$ nm [1–5]) while sustaining a sufficiently large signal-to-noise ratio (SNR) and thermal stability of written information withstanding the demagnetizing field for ten years [6]. This problem leads to the criterion $K_U V \geq 60 k_B T$, where K_U is the uniaxial anisotropy constant, V is the grain volume, k_B is Boltzmann's constant, and T is the temperature. The increasing values of K_U cause the writability of information to become an issue, and the conflicting requirements of stability, writability, and SNR have become known as the media trilemma [7].

There are several alternative approaches to overcome these limitations such as heat-assisted magnetic recording (HAMR) [8], a technology based on using a laser-delivered heat assist for the writing process on very high anisotropy materials, i.e., FePt alloys [1,9,10]. Moreover, bit-patterned media [11] and microwave-assisted magnetic recording [12] technologies have been also proposed as key ideas. Unfortunately, there are several limitations to these technologies, which are not only a type of write head design but also the nanofabrication process for industry. Therefore, new designs of conventional perpendicular recording media (PRM) are still the favored option, and perpendicular magnetic recording remains the only technology currently used in hard disk drives.

Conventional PRM have faced several problems, mainly with writability and SNR when the grain size decreases, requiring increasingly large values of K_U. In order to address these problems, there are two main composite media proposed. The first is exchange-coupled composite (ECC) media [13,14] consisting of a low anisotropy material which is known as the switching layer overlaid on a granular high anisotropy layer to reduce the switching field H_S via the magnetization-reversal mechanism. The second is coupled granular continuous (CGC) media [15–17] introducing the continuous layer to control intergranular exchange coupling, which can enhance the performance of the medium for high thermal stability and SNR.

Recently, a hybrid granular recording media design [18–20] has been introduced, combining the advantages of ECC and CGC media to improve the performance of recording media in order to achieve an areal density beyond 1 Tbit/in^2 in conventional perpendicular recording. The stacked structure of the design consists of a trilayer system comprising a hard layer, M_{L1} (very high K_U), a soft layer M_{L2}, and a continuous layer (M_{L3}) as a capping layer. The medium comprises small columnar grains which are completely segregated by SiO_2, while the continuous capping layer provides a highly uniform exchange coupling. The key advantage of the magnetic multilayer design

*jessada.c@msu.ac.th

is the high reduction of the switching field due to the presence of the ultrathin magnetic soft layer leading to dramatically improved writing efficiency and thermal stability. Moreover, the design feature of a continuous capping layer has a significant advantage by creating a strong pinning to achieve the narrow switching field distribution. In order to better understand the magnetization-reversal mechanisms behind the complex structure of PRM, the impact of the exchange coupling among the individual magnetic thin layers affecting to the reversal process and magnetic performance of the whole structure need to be exposed. Certainly, it is difficult to discover experimentally the detailed reversal processes of each layer in ultrathin magnetic film. Therefore, the atomistic spin simulation can describe the information on the magnetization-reversal process of each layer including the effect of intra- and interexchange coupling at the atomic level and also the demagnetizing field which are significant factors for perpendicular complex recording media. The effect of the magnetic parameters such as the uniaxial anisotropy, the atomic exchange interaction, and film thickness on magnetic properties of recording media can be studied. Meanwhile, the experimental work suffers to control these parameters. The atomistic model is a tool worth investigating to determine the factors affecting the performance of recording media before looking at the detail experimentally.

In previous experimental and theoretical works [21–25], it was reported that the presence of interactions media in granular and ECC media can lead to a deviation of the switching behavior, in particular, the angular dependence of magnetic properties, from the coherent Stoner-Wohlfarth theory [26]. Studies of the reversal process of such complex structures as ECC+CGC media are lacking and are still required in experiment and theory. Hence, it is important to investigate the effects of the complicated interaction as the hybrid ECC+CGC media in order to better understand the complex physics in such media design. Complex media with relatively thin layers are not necessarily amenable to micromagnetic calculations with a relatively crude spatial discretization. In this paper, atomistic spin simulation [27] based on the Landau-Lifshitz-Gilbert (LLG) equation of motion is chosen to study the complex reversal mechanisms for hybrid ECC+CGC media due to the reduction of the magnetic granular grain and the layer thickness almost to the atomic level. We show that the quantitative intra- or interexchange coupling between spins becomes very significant in terms of the reversal behavior. The magnetization curve and the angular dependence of the critical field $H_{\rm cr}$ are investigated to study the magnetic properties and the reversal process for the complex structure. The effect of time dependence on the switching field, which is significant for the writing process, is also studied in this work. Finally, we study the reversal behavior at field sweep rates comparable to those during the recording process. This is shown to give rise to a significant and irreducible contribution to the switching field distribution from thermal activation. It is important to note that the atomistic model becomes an important tool to investigate the complex behavior of magnetic nanomaterials. It will be very useful for other potential application areas as well. This model can be applied to further investigations of complex magnetic structure leading to not only the development of magnetic recording media leading to media architectures such as heat-assisted magnetic recording, bit-patterned media, and microwave-assisted magnetic recording media, but also other applications such as spintronics device designs, spin torque, surface anisotropy in magnetic nanoparticles, the exchange bias in spin valves of read elements, and the interface effect of nanomagnetic devices.

II. ATOMISTIC MODEL

An atomistic spin-dynamics model based on the LLG approach is used to investigate theoretically the magnetic properties of the ECC+CGC medium, including the angular dependence of the critical field ($H_{\rm cr}$) and the magnetization-reversal process for the advanced PRM. The energy of the system is described by a classical spin Hamiltonian with the parameters of the CoPt-based alloys commonly used as PRM. The spin Hamiltonian with the Heisenberg form of exchange is written for spin i as

$$\mathcal{H} = \mathcal{H}_{\rm exc} + \mathcal{H}_{\rm ani} + \mathcal{H}_{\rm app}, \tag{1}$$

where $\mathcal{H}_{\rm exc}$ is the exchange energy which is written in Heisenberg form as $\sum_{j\neq i} J_{ij}\mathbf{S}_i \cdot \mathbf{S}_j$. J_{ij} is the exchange coupling between the spin i and j, the sum running over nearest neighbors, and $\mathbf{S}_i$, $\mathbf{S}_j$ is the local normalized spin moment on sites i and j, respectively. $\mathcal{H}_{\rm ani}$ is the uniaxial magnetic anisotropy energy expressed as $k_U(\mathbf{S}_i \cdot \mathbf{e})^2$, where k_U is the uniaxial anisotropy constant per spin, and $\mathbf{e}$ is the unit vector of the easy-axis orientation. The last term of Eq. (1) is the energy of an external applied magnetic field, which is simply given by $-\mu_s \mathbf{S}_i \cdot \mathbf{H}_{\rm app}$, where $|\mu_s|$ is the magnitude of the spin moment, and $\mathbf{H}_{\rm app}$ is the external applied field. It is noted that the spin Hamiltonian ($\mathcal{H}$) is expressed as energies per atom and used to determine a field contribution at site i, $H_i = -\partial\mathcal{H}/\partial\mu_i$, where μ_i is the moment on site i. Furthermore, the thermal fluctuation field $\mathbf{H}_{\rm ther}$ is included by using Langevin dynamics in the formalism of Brown [28], converting the LLG into the (stochastic) Langevin equation of the problem. Finally, the dipolar field $\mathbf{H}_{\rm dip}$ is also taken into account in the atomistic model by using a macrocell technique developed by Boerner *et al.* [29]. The dipolar field is estimated by dividing the system into macrocells (MC). The demagnetization field within each macrocell p of moment $\mathbf{m}^q_{\rm MC}$ is given by

$$\mathbf{H}^{{\rm MC},p}_{\rm demag} = \frac{\mu_0}{4\pi}\left(\sum_{q\neq p}\frac{3(\mathbf{m}^q_{\rm MC}\cdot\hat{\mathbf{r}})\hat{\mathbf{r}} - \mathbf{m}^q_{\rm MC}}{r^3}\right) - \frac{\mu_0}{3}\frac{\mathbf{m}^q_{\rm MC}}{V^p_{\rm MC}}, \tag{2}$$

where r is the separation between dipoles p and q, $\hat{\mathbf{r}}$ is a unit vector in the direction $p \rightarrow q$, and V_{MC}^{p} is the volume of the macrocell p. The first term in Eq. (2) is the usual dipole term arising from all *other* macrocells in the system, while the second term is the self-demagnetization field of the macrocell taken here as having a demagnetization factor ⅓. Further details of the $\mathbf{H}_{\mathrm{ther}}$ and $\mathbf{H}_{\mathrm{dip}}$ calculations can be found in Refs. [27,30]. Finally, the total field or the net effective local field $\mathbf{H}_{\mathrm{eff}}^{i}$ acting on each spin is the summation of the negative first derivative of the spin Hamiltonian including the effect of the thermal field and dipolar field expressed as

$$\mathbf{H}_{\mathrm{eff}}^{i} = -\frac{1}{\mu_s}\frac{\partial \mathcal{H}}{\partial \mathbf{S}_i} + \mathbf{H}_{\mathrm{dip}} + \mathbf{H}_{\mathrm{ther}}. \quad (3)$$

The dynamic motion of magnetization in advanced PRM at the atomic level is determined by using a LLG approach. This equation consists of the precessional term of the normalized spin moment around the effective field and the spin-relaxation term which is controlled by the damping parameter λ in the damping term of the LLG equation, which is given by

$$\frac{\partial \mathbf{S}_i}{\partial t} = -\frac{\gamma}{(1+\lambda^2)}[\mathbf{S}_i \times \mathbf{H}_{\mathrm{eff}}^{i} + \lambda \mathbf{S}_i \times (\mathbf{S}_i \times \mathbf{H}_{\mathrm{eff}}^{i})], \quad (4)$$

where $\mathbf{S}_i$ is the unit vector of the spin moment i to represent the direction of spin, γ is the gyromagnetic ratio, and λ is the Gilbert damping constant which is used as 1.0 for this system. We note that all atomic simulations are done using the VAMPIRE software package [27].

III. ECC+CGC RECORDING MEDIA DESIGN

The structure of the ECC+CGC recording medium is designed with a trilayer system to drive a high areal density beyond 1 TB per square inch with a high anisotropy constant (H_k) and small grains. The aim is to achieve a medium with reduced coercivity while minimizing the reduction of the zero-field energy barrier responsible for long-term stability. The details of the material parameters used in our atomistic spin-dynamics calculation are determined experimentally for the future granular recording media which are provided by Seagate Technology of Fremont. Because of this calculation based on the spin Hamiltonian shown as Eq. (1), the magnetic parameters such as anisotropy constant k_U, saturation magnetization, and exchange inter- and intralayer coupling are necessary to parametrize in terms of the atomic level. The trilayer media design consists of a storage layer with a high anisotropy field H_{k1} of 22 kOe, the uniaxial anisotropy constant $k_{U1} = 5 \times 10^{-23}$ J/atom, saturation magnetization $M_s = 4.4\mu_B$ (700 emu/cc), and a thickness of 21 atomic layers (approximately 7 nm). The second layer is a softer layer with a lower H_{k2} of 16 kOe, $k_{U2} = 4.2 \times 10^{-23}$ J/atom, $M_s = 5\mu_B$ (800 emu/cc), and a thickness of

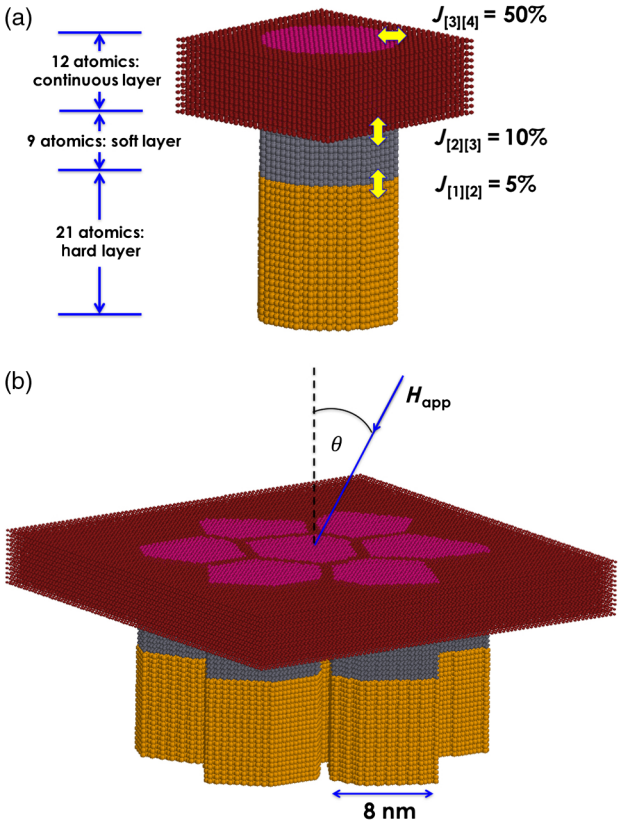

FIG. 1. (a) A single-grain structure. (b) The few-grain structure for advanced media design.

nine atomic layers (approximately 3 nm). The third layer is the continuous capping layer, the granular medium having the lowest H_{k3} of 10 kOe, $k_{U3} = 2 \times 10^{-23}$ J/atom, $M_s = 3.8\mu_B$ (600 emu/cc), and a thickness of 12 atomic layers (approximately 4 nm). It is noted that our magnetic parameters used in this work agree well with the previous experimental works for future granular recording media with HAMR and MAMR technologies reported by Saito *et al.* [31] and Tham *et al.* [32,33].

The composite materials for all layers are based on a common CoPt-based alloy with the Curie temperature of 1000 K. The grain size of the first and second layers is set as 8 nm with wide nonmagnetic grain boundaries of 1 nm in order to remove the intergranular exchange coupling. The top layer is modeled as a continuous film with no grain boundaries in which the exchange intralayer coupling is set at 50% of J_{ij}, where J_{ij} is the exchange-coupling strength between atoms $J_{ij} = 9.86 \times 10^{-21}$ J/link. Meanwhile, the exchange interlayer coupling strength between the first and second layers and second and third layers is set at 5% and 10% of J_{ij}, respectively. Figures 1(a) and 1(b) present a visualization of the atomic structure of a single grain (approximately 23 000 atoms) and few grains (approximately 175 000 atoms) with 1.0-nm spacing, respectively, employed to examine the impact of media architectures

on the magnetization-reversal process and the angular-dependent critical field.

IV. MAGNETIC CHARACTERIZATION

We present an investigation of the magnetic properties of hybrid EEC CGC media, first showing the basic hysteretic behavior. In the following, the magnetic properties are calculated using the atomic model for two cases: first, a small system comprising seven grains using a $34 \times 34 \times 16$ nm^3 system as Fig. 1(b), and second, a multigrain structure using a $50 \times 50 \times 16$ nm^3 system containing 27 grains.

In order to investigate the magnetic properties of ECC CGC composite media, we first show a typical hysteresis loop for the small system at an angle between the applied field and the normal direction to the film plane $\theta = 0°$. Hysteresis loops are calculated for a reversal time of 20 ns. The impacts of the dipolar field and thermal activation are investigated. Figure 2 shows the normalized hysteresis loops with and without the dipolar field at 0 K for the ECC CGC medium described earlier. It is clear that the $\mathbf{H}_{\mathrm{dip}}$ has a significant effect on the magnetic properties, especially the coercivity H_c. The value of H_c reduces significantly from 15 to 10 kOe on inclusion of the dipolar field. The result shows the strong impact of dipolar field on coercivity due to the effect of the large demagnetizing field reversing the continuous layer for the ECC+CGC structure. The reduction essentially arises from the onset of a nucleation and propagation mechanism driven by the dipolar field. This is investigated later in detail with the comparative visualization of the reversal process with and without $\mathbf{H}_{\mathrm{dip}}$.

Moreover, the composite design of the trilayer structure can improve the performance of recording media, as expected. The hysteresis loop in Fig. 2 shows a significant reduction of the switching field to a value of H_c of 10 kOe, while the H_k of the hard or storage layer is a very high value of 22 kOe. The results also indicate the effect of the parameters used in the model. The reduction of H_c is probably due to the presence of the softer layer with a low anisotropy constant and a low exchange interlayer coupling (5% of J_{ij}). Moreover, the shape of the hysteresis loop is very square due to the presence of the third layer with a strong intralayer coupling strength (50% of J_{ij}). This result coupled with the effects of the saturation magnetization and anisotropy of the layers means that a complete optimization of the media properties is beyond the scope of the current work. The optimization of the properties is probably best done by using the atomistic approach to parametrize simplified models, possibly with one spin per layer, in order to lower the computational cost. Here, we concentrate on developing an understanding of the basic reversal mechanisms involved, including the effects of interactions, of which an investigation follows.

We now turn to the set of interacting grains. The initial hysteresis loop calculations are made using the small system of seven grains; this is due to the necessity of long run times to achieve equilibrium loops. Figure 3 shows the impact of the thermal activation at 300 K on the loops and coercivity in comparison with the 0-K behavior with the reversal of each individual layer as an inset. The thermal energy directly reduces the value of the coercivity and saturation magnetization of the whole system. However, it does not affect the form of the hysteresis loop, which remains very square in both cases. Moreover, information on the magnetization-reversal process can be obtained from the net magnetization curve of each layer. The insets of Fig. 3 show the layer-resolved magnetization behavior as M_{L1} (hard layer), M_{L2} (soft layer), and M_{L3} (continuous layer) around the switching state at a field H_s and temperature of 0 K (top) and 300 K (bottom). The results for both temperatures display similar behavior. The H_S of the M_{L1} layer is the highest value, while the H_S of M_{L2} is slightly higher than the top layer M_{L3} at the reversal state.

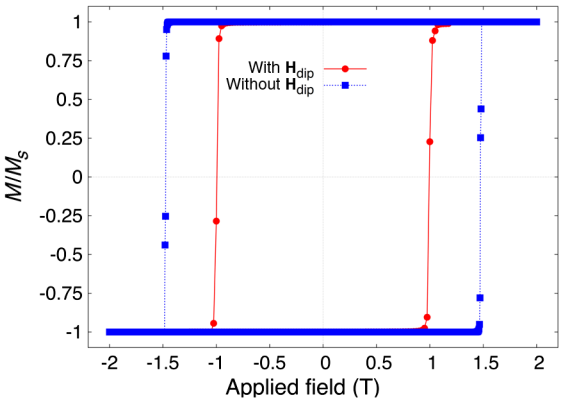

FIG. 2. Hysteresis loops of a single-grain structure with and without dipolar interaction showing the dipole field gives rise to a significant reduction in coercivity.

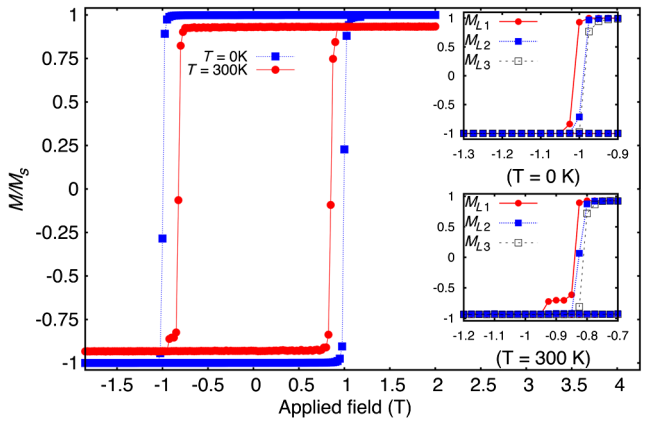

FIG. 3. Hysteresis loop measured at 0° with $\mathbf{H}_{\mathrm{dip}}$ and calculated with a reversal time of 20 ns at different temperatures. The insets show the magnetization curve of each magnetic layer around the H_S at $T = 0$ (top) and 300 K (bottom).

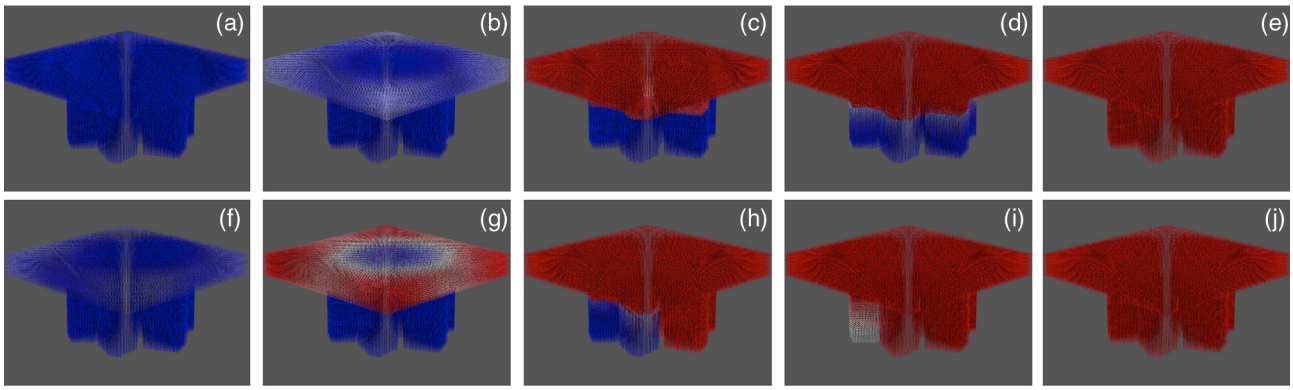

FIG. 4. Visualization of atomic magnetization reversal for the few-grain system at $T = 0$ K and 0° for exclusion of $\mathbf{H}_{\mathrm{dip}}$ (a)–(e) and inclusion of $\mathbf{H}_{\mathrm{dip}}$ (f)–(j).

This indicates that the reversal process probably initiates in the top layer and propagates through the bottom layer. This is confirmed by the visualization of the switching process at the atomic level as shown in Fig. 4, where the nucleation and propagation can clearly be seen. An interesting feature of the inset of Fig. 3 is the step in magnetization observable close to saturation in the negative-going loop at $T = 300$ K. This result is associated with the late switching of one of the grains due to stabilization of the positively oriented grain by the magnetostatic field.

The effect of the magnetostatic interaction field on the reversal behavior for hybrid ECC+CGC media referred to earlier is further investigated by observation of the atomic reversal process for the few-grain system. Figure 4 displays the visualizations of the atomistic reversal process for the exclusion and inclusion the magnetostatic field, respectively, at 0 K. For the exclusion of $\mathbf{H}_{\mathrm{dip}}$ case, Figs. 4(a)–4(e) show the subsequent reversal process of each layer. The top layer initially reverses when the applied field is higher than H_{k3}. Subsequently, the whole stack of continuous layers and soft layers reverses followed finally by the hard layer. For the case including $\mathbf{H}_{\mathrm{dip}}$ as shown in Figs. 4(f)–4(j), it is clearly seen that the partial region of the top layer reverses initially. This is due to the strong effect of the dipolar field to initiate a collective nucleation and propagation mechanism, especially on a continuous layer having a high exchange-coupling interaction. The reversal of spins is transmitted to neighboring spins leading to the reversal of all grains almost simultaneously. This result may cause the reduction of the coercivity and confirms that the dipolar field becomes an important factor for the magnetic properties of complex recording media. We note that Fig. 4 shows a subtle effect of the magnetostatic field on the reversal mechanism. A comparison between Figs. 4(a)–4(e) and 4(f)–4(j) shows that the reversal is much more uniform in the absence of the magnetostatic field. Figures 4(a)–4(e) show similar time propagation of reversal in each of the grains, whereas Figs. 4(f)–4(j) show that individual grains switch at different times. This result is an effect which we attribute to spatial variations of the magnetostatic field arising from slight differences in the grain morphology and which could contribute to the width of the thermal switching field distribution (SFD) that we describe later.

V. ANGULAR DEPENDENCE OF H_{cr}

One of the main aims of this work is to understand the switching behavior of the multilayer structure. The inclusion of the magnetostatic interaction field is taken into account in the atomistic calculation to demonstrate its significant effect on the magnetic properties. The angular dependence of the critical field H_{cr} defined as the field at which the magnetization flips irreversibly from one stable state to another is used to investigate the reversal process. The influence of thermal effects at room temperature 300 K is modeled by including the thermal fluctuation field H_{ther}. In this atomistic calculation, the magnetic properties of each layer such as the magnetocrystalline anisotropy field, layer thickness, grain diameter, and exchange inter- or intralayer coupling are given in Sec. III. All calculations are done for the small (seven-grain) system.

The normalized hysteresis loop is calculated as a function of θ ranging from 0° to 90° with the field step of 5° in order to explore H_{cr}. The angular dependence of the critical field is calculated with and without magnetostatic interactions at temperatures of 0 and 300 K. Figures 5(a) and 5(b) demonstrate typical hysteresis loops at 0 K for the angular ranges of 0° to 45° and 50° to 90°, respectively. The loops are calculated for a reversal time of 20 ns. The results show that the H_{cr} has a maximum value at 0° and reduces to a minimum value with increasing angle at 45°. Subsequently, the critical field increases as the angle approaches 90°. It is interesting to note that the hysteresis loops without H_{dip} for large angles display the crossover effect resulting from irreversible switching between minima as shown in Fig. 5(b). This feature and the general form of the switching behavior suggest that in the absence of magnetostatic interaction the magnetization reverses coherently as the Stoner-Wohlfarth

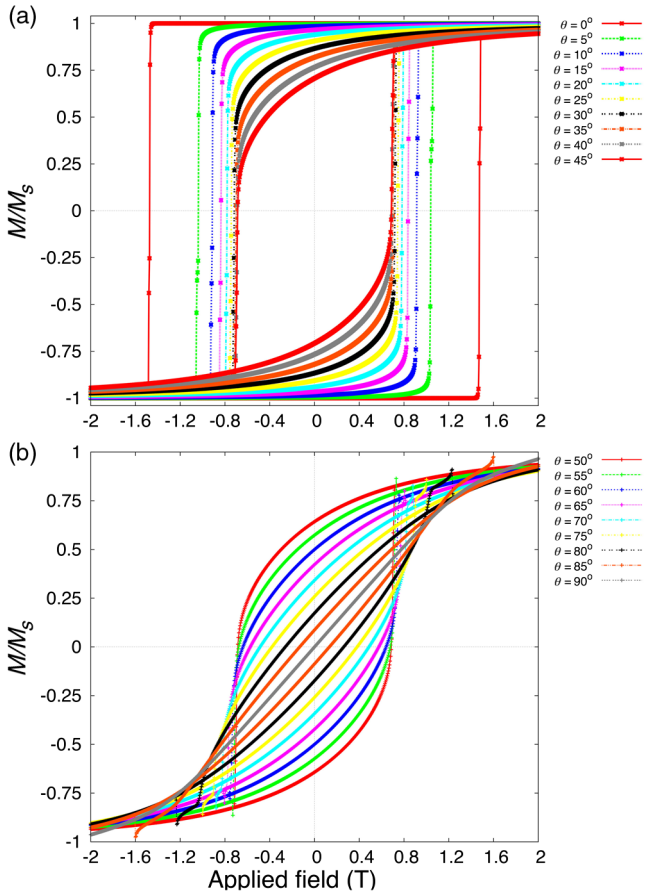

FIG. 5. The typical hysteresis loops at 0 K calculated for a reversal time of 20 ns without the inclusion of magnetostatic interactions: (a) the angular ranges from 0° to 45° and (b) from 50° to 90°.

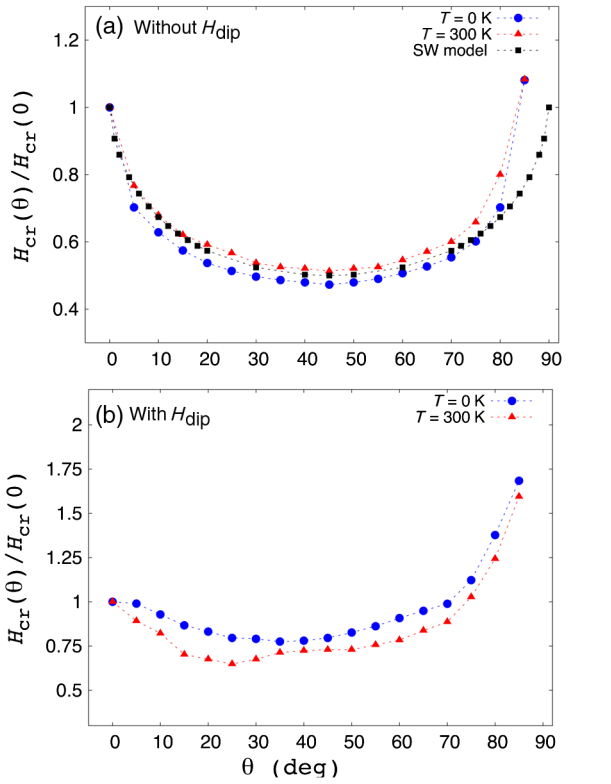

FIG. 6. Variation of the normalized critical field $H_{cr}(\theta)/H_{cr}(0)$ as a function of angle and temperature (0 and 300 K). (a) No H_{dip} effect and (b) including H_{dip} effect.

behavior [26] as observed and reported by Tannous and Gieraltowski [34].

Calculations of the $H_{cr}(\theta)$ normalized by $H_{cr}(\theta = 0)$ as a function of the applied field angle θ are performed at 0 and 300 K to determine the magnetization-reversal mechanism. In order to investigate the effects of the magnetostatic interaction field and thermal activation on the switching process, comparisons of the variation of the normalized $H_{cr}(\theta)/H_{cr}(0)$ with angles are shown in Fig. 6 for calculations with and without the magnetostatic interaction field.

Figure 6(a) shows the angular dependence of H_{cr} for the noninteracting case for both temperatures. It is clearly observed that the minimum of the critical field is close to half the $H_{cr}(0)$ value at 45° for both absolute temperatures. The change of the normalized H_{cr} with the angle shows the similar behavior of the Stoner-Wohlfarth theory [26], also included in Fig. 6(a), for both temperatures, which is a good indication of coherent magnetization reversal for the system without magnetostatic fields. Further evidence can be observed from the visualization of the atomic reversal process given in Figs. 4(a)–4(e). However, coherent reversal behavior is not expected to occur in such a complex structure [23,24], suggesting that noncoherent behavior is induced by magnetostatic interactions.

We now proceed to investigate the angular dependence of H_{cr} for more realistic calculations by including the effect of the magnetostatic interaction field into the system. Interestingly, it is found that the inclusion of interactions strongly influences the reversal mechanism of the ECC +CGC media observed from the transformation of the variation of H_{cr} in Fig. 6(b). The trend of angular dependence for both temperatures shows that the reversal behavior clearly deviates from coherent Stoner-Wohlfarth theory [26]. The curve is asymmetric with minimum critical field at 35° and 25° for $T = 0$ and 300 K, respectively. The form of the variation is closer to the characteristic of domain-wall motion initiated and driven by the magnetostatic interaction.

The trend of the variation of H_{cr} with the angle demonstrates the incoherent magnetization reversal during the switching process. The incoherent reversal causes the appearance of several reversal modes such as cooperative reversal between grains, collective nucleation, and propagation and pinning at the interface layer due to the lateral exchange interaction. This outcome can be clearly seen in Figs. 4(f)–4(j). The continuous layer starts to reverse as an incoherent reversal process. The continuous layer initiates a collective domain-wall nucleation due to the strong exchange between layers. Magnetization reversal in the granular layer cannot occur

until the domain wall propagates through the bottom as in Figs. 4(h)–4(j). This reversal behavior is completely different from the Stoner-Wohlfarth (SW) model [26]. Significantly, the results confirm that the magnetostatic interaction effect is the crucial factor driving the reversal behavior for complicated advanced recording media in simulation, which cannot be neglected.

Figure 6 must be considered alongside the nature of the switching, as illustrated by the transient magnetization configurations shown in Fig. 4. Figure 6(a) apparently shows classic SW behavior; however, inspection of Figs. 4(a)–4(e) shows that reversal is proceeded by nucleation and propagation. A possible interpretation of this is that nucleation involves a similar form of energy barrier as the SW model. Investigation of this prospect will be interesting, but it requires the calculation of energy barriers using the constrained Monte Carlo method [35], which is beyond the scope of the current work. As expected, the magnetostatic field has a strong bearing on the reversal mechanism. Figure 6(b) shows an angular variation consistent with domain-wall nucleation and propagation. However, as noted earlier, the transient states shown in Fig. 4(f)–4(j) show individual grain reversal at different times. It seems likely that this is an important contribution to the thermal SFD that we consider shortly.

Moreover, our angular-dependence calculations agree well with the previous experimental works which observed the irreversible behavior of advanced recording media. The variation of the H_{cr} technique was used by Saharan *et al.* [23,24] to study the magnetization-reversal behavior in a trilayer structure based on exchange spring media [13] separated with the additional interface layer. They found that the minimum angle of the critical field is about 30°–35°, which is consistent with our calculations for hybrid media design including the magnetostatic field case. The similar trend of variation of H_{cr} with the angle of the segregated granular recording based on CoCrPt-SiO_2 media is also observed experimentally by Morrison *et al.* [25]. They found that the asymmetry of the variation of the critical field and the breakdown of Stoner-Wohlfarth behavior occurred in cases of strong magnetostatic field and weak exchange coupling.

VI. TIME DEPENDENCE OF H_c IN ECC+CGC MEDIA

A critical parameter in advanced recording media is the switching field of the medium. The significant feature of this field is the time or frequency dependence of the switching field described by the well-known Sharrock equation [36,37] as

$$H_c(t) = H_K\left\{1 - \left[\frac{k_B T}{K_U V}\ln\left(\frac{f_o t}{0.693}\right)\right]^n\right\}, \qquad (5)$$

where $H_c(t)$ is the time dependence of the coercivity, t is the time scale, H_K is the anisotropy field, and f_o is a frequency factor. From the Sharrock equation, short time scales give rise to large values of the switching field.

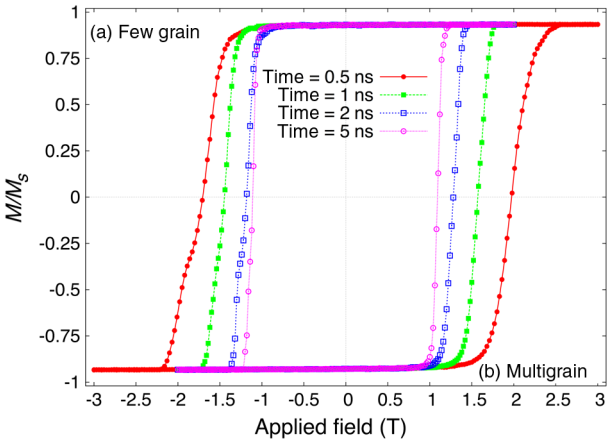

FIG. 7. Half-hysteresis-loop (a) few-grain system (half left) and (b) multigrain system (half right) as a function of different loop times 0.5, 1, 2, and 5 ns at 300 K.

Of particular importance is the fact that the writing process operates at extremely high frequency (gigahertz) or short time scale (<0 ns) [37]. Consequently, the write field must be larger than the switching field at the write frequency.

The time dependence of H_c is investigated for both small and multigrain systems as a function of the different loop times of 0.5, 1, 2, and 5 ns with the external field applied normal to the plane at 300 K. The aim of this investigation is to study the properties of the system in the transition region into the subnanosecond time scale of magnetic recording. In particular, we are interested in the form of the hysteresis loop and also the thermal SFD [38], which represents an irreducible minimum SFD for the system. For computational efficiency, the small system is used for initial investigations, and the multigrain structure is used for the detailed calculations of the thermal switching field distribution that we describe later.

Figures 7(a) and 7(b) show the half (left) hysteresis loop for the small system and the half (right) hysteresis loop for the multigrain system at the different loop times, respectively. The results for both systems exhibit the expected significant reduction of coercivity with increasing loop time, which is consistent with the Sharrock equation. The value of H_c is similar at each loop time for both systems. There is an obvious kink in the magnetization curve at a short loop time for the seven-grain system, which disappears for the multigrain system due to more statistical data. The feature arises from the tendency noted earlier for delayed switching of some grains; it leads to a kink in the small system but a smooth magnetization curve for the multigrain case.

Finally, the SFD is calculated from the gradient of the magnetization curve and presented for the different loop times in Fig. 8. The results show that a reduction of the loop time significantly increases the SFD. According to the SFD width (σ_{SFD}), the inset of Fig. 8 shows the decreasing of σ_{SFD} with the increasing of the loop time. This effect arises from the reduction of the energy barrier at which switching

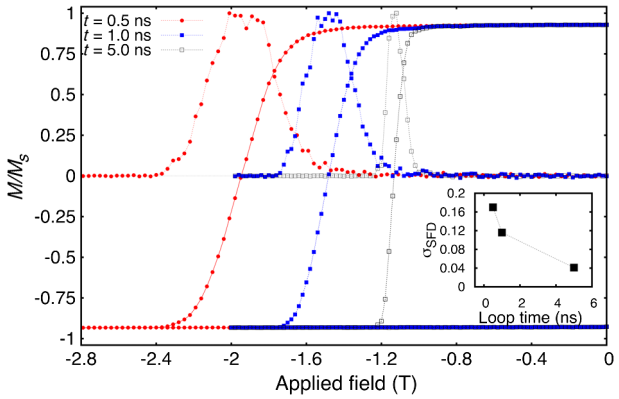

FIG. 8. Switching field distribution obtained at different loop times 0.5, 1, and 5.0 ns by differentiation of the hysteresis loop, and the inset shows the SFD width σ_{SFD} versus loop times.

occurs for small reversal times [38], which broadens the field dependence of the switching probability.

VII. CONCLUSION

In this work, we perform atomistic calculations based on the Landau-Lifshitz-Gilbert equation of motion to study the magnetic properties and the magnetization-reversal behavior of the composite trilayer system as advanced recording media. The design of hybrid granular recording media [18–20] is introduced using the advantage of ECC and CGC media. The structure of the medium consists of a trilayer system of a hard layer, soft layer, and continuous layer. From magnetic characterization, the hybrid ECC+CGC media demonstrate the enhancements of the recording performance such as thermal stability and SNR by reducing the switching field and narrowing the switching field distribution.

The variation of the critical field as a function of applied field angle is investigated to understand the magnetization-reversal mechanism. We also report a significant effect of the magnetostatic interaction field on the simulation. The inclusion of H_{dip} is taken into account in the atomistic calculation to demonstrate its strong effect on the reversal process of a realistic system. The feature of the angular dependence of H_{cr} without the effect of H_{dip} shows the coherent reversal behavior like the Stoner-Wohlfarth model [26], which does not describe the mechanism of a complex structure. Meanwhile, the calculations, including the effect of H_{cr}, indicate the incoherent reversal process due to the appearance of several complex reversal modes. Therefore, it confirms that the magnetostatic interaction field is a crucial factor which cannot be neglected for simulations to reveal realistic properties.

ACKNOWLEDGMENTS

J. C. gratefully acknowledges financial support from Division of Research, Mahasarakham University, Thailand and Development and Promotion of Science and Technology Talents (DPST) Research Grant No. 23/2557.

[1] S. Piramanayagam and K. Srinivasan, Recording media research for future hard disk drives, J. Magn. Magn. Mater. **321**, 485 (2009).
[2] J. Chureemart, P. Chureemart, R. Evans, R. W. Chantrell, and K. O'Grady, Magnetic orientation in advanced recording media, J. Phys. D **44**, 455002 (2011).
[3] J. Chureemart, L. Lari, T. P. Nolan, and K. O'Grady, The effect of SiO_2 content on activation volumes in exchange coupled composite media, J. Appl. Phys. **114**, 083907 (2013).
[4] V. Mehta, T. Wang, Y. Ikeda, K. Takano, B. D. Terris, B. Wu, C. Graves, H. A. Durr, A. Scherz, J. Stohr, and O. Hellwig, Extracting magnetic cluster size and its distributions in advanced perpendicular recording media with shrinking grain size using small angle x-ray scattering, Appl. Phys. Lett. **106**, 202403 (2015).
[5] C. Papusoi, M. Desai, and R. Acharya, Evaluation of intergranular exchange coupling and magnetic domain size in CoCrPt-SiO_x thin films with perpendicular anisotropy, J. Phys. D **48**, 215005 (2015).
[6] S. Charap, P.-L. Lu, and Y. He, Thermal stability of recorded information at high densities, IEEE Trans. Magn. **33**, 978 (1997).
[7] H. J. Richter, The transition from longitudinal to perpendicular recording, J. Phys. D **40**, R149 (2007).
[8] R. Rottmayer, S. Batra, D. Buechel, W. Challener, J. Hohlfeld, Y. Kubota, L. Li, B. Lu, C. Mihalcea, K. Mountfield, K. Pelhos, C. Peng, T. Rausch, M. A. Seigler, D. Weller, and X. Yang, Heat-assisted magnetic recording, IEEE Trans. Magn. **42**, 2417 (2006).
[9] D. Weller, O. Mosendz, G. Parker, S. Pisana, and T. S. Santos, $L1_0$ FePt*X*-*Y* media for heat-assisted magnetic recording, Phys. Status Solidi A **210**, 1245 (2013).
[10] S. Granz, K. Barmak, and M. Kryder, Granular $L1_0$ FePt:*X* (X = Ag, B, C, SiO_x, TaO_x) thin films for heat assisted magnetic recording, Eur. Phys. J. B **86**, 81 (2013).
[11] B. D. Terris and T. Thomson, Nanofabricated and self-assembled magnetic structures as data storage media, J. Phys. D **38**, R199 (2005).
[12] J. G. Zhu, X. Zhu, and Y. Tang, Microwave assisted magnetic recording, IEEE Trans. Magn. **44**, 125 (2008).
[13] R. Victora and X. Shen, Composite media for perpendicular magnetic recording, IEEE Trans. Magn. **41**, 537 (2005).
[14] D. Suess, T. Schrefl, S. Fahler, M. Kirschner, G. Hrkac, F. Dorfbauer, and J. Fidler, Exchange spring media for perpendicular recording, Appl. Phys. Lett. **87**, 012504 (2005).
[15] Y. Sonobe, D. Weller, Y. Ikeda, M. Schabes, K. Takano, G. Zeltzer, B. Yen, M. E. Best, S. Greaves, H. Muraoka, and Y. Nakamura, Thermal stability and SNR of coupled granular/continuous media, IEEE Trans. Magn. **37**, 1667 (2001).
[16] G. Choe, M. Zheng, B. R. Acharya, E. N. Abarra, and J. N. Zhou, Perpendicular recording CoPtCrO composite media with performance enhancement capping layer, IEEE Trans. Magn. **41**, 3172 (2005).
[17] J. Yasumori, Y. Sonobe, S. J. Greaves, and K. K. Tham, Approach to high-density recording using CGC structure, IEEE Trans. Magn. **45**, 850 (2009).
[18] T. P. Nolan, B. F. Valcu, and H. J. Richter, Effect of composite designs on writability and thermal stability of perpendicular recording media, IEEE Trans. Magn. **47**, 63 (2011).

[19] K. K. Tham, S. Saito, D. Hasegawa, N. Itagaki, S. Hinata, S. Ishibashi, and M. Takahashi, Effect of inhomogeneous microstructure of granular layer on inter granular/inter layer exchange coupling in stacked perpendicular recording media, J. Appl. Phys. **112**, 093917 (2012).

[20] J. Chureemart, P. Chureemart, J. Pressesky, T. Nolan, and K. O'Grady, Media design and orientation in perpendicular media, IEEE Trans. Magn. **49**, 3592 (2013).

[21] C. Morrison, L. Saharan, G. Hrkac, T. Schrefl, Y. Ikeda, K. Takano, J. J. Miles, and T. Thomson, Inter/intra granular exchange and thermal activation in nanoscale granular magnetic materials, Appl. Phys. Lett. **99**, 132507 (2011).

[22] L. Saharan, C. Morrison, J. J. Miles, T. Thomson, T. Schrefl, and G. Hrkac, Angle dependence of the switching field of recording media at finite temperatures, J. Appl. Phys. **110**, 103906 (2011).

[23] L. Saharan, C. Morrison, Y. Ikeda, K. Takano, J. J. Miles, T. Thomson, T. Schrefl, and G. Hrkac, Grain boundaries in granular materials–A fundamental limit for thermal stability, Appl. Phys. Lett. **102**, 142402 (2013).

[24] L. Saharan, C. Morrison, J. J. Miles, T. Thomson, T. Schrefl, and G. Hrkac, Modelling interfacial coupling in thin film magnetic exchange springs at finite temperature, J. Appl. Phys. **114**, 153908 (2013).

[25] C. Morrison, L. Saharan, Y. Ikeda, K. Takano, G. Hrkac, and T. Thomson, Quantifying exchange coupling in segregated granular materials, J. Phys. D **46**, 475002 (2013).

[26] E. C. Stoner and E. P. Wohlfarth, A mechanism of magnetic hysteresis in heterogeneous alloys, Phil. Trans. R. Soc. Lond. **240**, 599 (1948).

[27] R. F. L. Evans, W. J. Fan, P. Chureemart, T. A. Ostler, M. O. A. Ellis, and R. W. Chantrell, Atomistic spin model simulations of magnetic nanomaterials, J. Phys. Condens. Matter **26**, 103202 (2014).

[28] W. F. Brown, Thermal fluctuations of a single-domain particle, J. Appl. Phys. **34**, 1319 (1963).

[29] E. Boerner, O. Chubykalo-Fesenko, O. Mryasov, R. Chantrell, and O. Heinonen, Moving toward an atomistic reader model, IEEE Trans. Magn. **41**, 936 (2005).

[30] P. Chureemart, R. F. L. Evans, and R. W. Chantrell, Dynamics of domain wall driven by spin-transfer torque, Phys. Rev. B **83**, 184416 (2011).

[31] S. Saito, S. Hinata, and M. Takahashi, Evaluation of atomic layer stacking structure and Curie temperature of magnetic films for thermally assisted recording media (invited), IEEE Trans. Magn. **50**, 102 (2014).

[32] K. K. Tham, S. Hinata, S. Saito, and M. Takahashi, Successful fabrication of high K_u columnar CoPt-SiO_2 granular film sputtered under high substrate temperature, J. Appl. Phys. **115**, 17B752 (2014).

[33] K. K. Tham, S. Hinata, and S. Saito, Effect of topological bumpy surface underlayer on compositionally modulated atomic layer stacking in high K_u hcp $Co_{80}Pt_{20}$ film with (00.2) crystallographic texture orientation, IEEE Trans. Magn. **51**, 3202404 (2015).

[34] C. Tannous and J. Gieraltowski, The Stoner-Wohlfarth model of ferromagnetism: Static properties, Eur. J. Phys. **29**, 475 (2008).

[35] P. Asselin, R. F. L. Evans, J. Barker, R. W. Chantrell, R. Yanes, O. Chubykalo-Fesenko, D. Hinzke, and U. Nowak, Constrained Monte Carlo method and calculation of the temperature dependence of magnetic anisotropy, Phys. Rev. B **82**, 054415 (2010).

[36] M. Sharrock and J. McKinney, Kinetic effects in coercivity measurements, IEEE Trans. Magn. **17**, 3020 (1981).

[37] M. P. Sharrock, Time dependence of switching fields in magnetic recording media (invited), J. Appl. Phys. **76**, 6413 (1994).

[38] O. Hovorka, R. F. L. Evans, R. W. Chantrell, and A. Berger, Rate-dependence of the switching field distribution in nanoscale granular magnetic materials, Appl. Phys. Lett. **97**, 062504 (2010).